

REACTION KINETICS AT LINEARLY INCREASED TEMPERATURE. III. INITIAL TEMPERATURES AND HEIGHTS OF PEAKS IN CONCENTRATION SERIES *

E. KOCH

*Max-Planck-Institut für Strahlenchemie, Stiftstr. 34–36, D-4330 Mülheim a.d. Ruhr
(West Germany)*

(Received 28 November 1983)

ABSTRACT

For reactions in solution, the readily available initial temperatures and heights of the DTA peaks of experimental concentration series give a first insight into the prevailing reaction mechanism.

The results for ten various systems studied show dramatic differences in the correlation of maximum signal height, referred to the concentration of varied reactants vs. initial temperature. The different types of such a correlation are discussed both for isolated and overlapping peaks, under inclusion of consecutive faster processes.

INTRODUCTION

Detailed evaluation and discussion of thermoanalytic signals of complex reactions requires the assumption of a suitable model—which in an early stage may be an elementary process [1]—and calculation of rates and activation energies, needing a certain mathematical effort [2]. However, if the signals are partially separated and not all reaction steps involved are of first order, then preliminary kinetic information may be available from two quantities to be obtained directly for each peak of a DTA curve or rate-related curve:

- (1) maximum signal height (v_m or θ_m), referred to the reactant concentration considered ($= v_{rel}$ or, for DTA, θ_{rel});
- (2) initial temperature T_0 , referred to a small standard fraction of the absolute maximum signal height, e.g., 0.5%.

If series of experiments are considered where one of the reactant starting concentrations is varied, but the others are held constant [3–5], both quanti-

* Presented, in part, at the Joint Nordic–German Symposium on Thermal Analysis and Calorimetry, 24–26 August 1983, Copenhagen, Denmark.

ties must show characteristic trends which can be summarized in a diagram T_0 (= abscissa) vs. θ_{rel} (or v_{rel}) using the initial concentration of the varied reactant ($a_0, b_0, c_0 \dots$) as a parameter. The often striking differences of such plots evolve from the fact that for a first-order process both values are constant, but for bimolecular processes they are not; then the signal measured is shifted on the temperature axis, because the second reactant appears to have a concentration-dependent rate coefficient. Thus, a negative shift of the onset is observed, whereas the whole signal becomes somewhat narrower [6], and, because of constant area, higher.

More complicated kinetic series for an isolated peak of a complex reaction were presented and discussed recently [7,8]. In the present paper, the results of various experiments are discussed under the inclusion of overlapping peaks [2,4].

EXPERIMENTAL

DTA concentration series of ten different reacting systems [2] were performed with our DTA solution equipment [9]; usually at a heating rate of 1.5 K min^{-1} . The systems involve reactants available commercially or by simple syntheses (Table 1).

In order to test a first-order process, aniline was diazotized, yielding benzenediazoniumsulfate as a reactant.

For each series, the starting concentration of one of the reactants was varied from experiment to experiment over a range of at least one order of magnitude, often beginning near that range where the signal onset surpassed the noise level, but ending before such high values occurred that a strong thermal feedback causing too strong temperature inhomogeneities or even a thermal explosion would have been expected [10]. The on-line evaluation procedure described earlier [2,10] is based on subtraction of an extrapolated baseline from the experimental DTA curve. The latter is exposed to a data reduction from ~ 2000 to ~ 150 points and, subsequently, to a soft smoothing algorithm of Sawitzky/Goley using a polynomial of 3rd order [11]. The resulting parametric T_0/θ_{rel} plots are summarized in Fig. 1. The particular experiments were mostly performed selecting concentration values stepped according to the 1-2-5-10 system. They are represented as points, and the lowest and highest starting concentrations are given in Table 1. The T_0 -scales of the series in Fig. 1 were taken, using the same T_0 -difference of 30 K in order to compare the absolute ranges. The relative sensitivity limit was chosen as 0.5% which is a realistic measure for the onset of the signal on normal chart paper or on a terminal.

In non-isothermal reaction analysis [8], the dependences of some simply measurable values on the reactant concentrations—and, even, on the heating rate [12,13]—are better represented by the logarithm of the concentration (or

TABLE 1

Results of DTA experiments in solution from concentration series^a

Cf. Fig. 1	System ^b (solvent)	Number of expts.	Conc. range		T_{av} (K)	$\frac{\log(\theta_{(max)})/\theta_{(min.)}}{\log C_{0(rat)}}$	$\frac{T_{0(max)} - T_{0(min)}}{\log C_{0(rat)}}$
			$C_{0(min)}$	$C_{0(max)}$			
a	Aniline + 6 NaNO ₂ (1.2 M H ₂ SO ₄)	8	0.03	0.6	300	0.10	2.5
b	Aniline + NaNO ₂ (1:1) (1.2 M H ₂ SO ₄)	7	0.02	0.6	301	0.08	3.4
c	NaBrO ₃ + 0.0345 NaBr + 0.0063 ferrioin + 0.375 MA (1.2 M H ₂ SO ₄)	9	0.005	0.12	330	0.56	5.1
d	NaIO ₃ + 0.58 H ₂ O ₂ (H ₂ O)	21	0.0025	0.06	320	1.69	7.5
e	0.025 Ce(SO ₄) ₂ + MA (1.5 M H ₂ SO ₄)	12	0.0025	0.375	268	1.30	~3
f	KMnO ₄ + 0.075 MA (H ₂ O)	15	0.0025	0.6	298	0.14	3.2
g	NaBrO ₃ + 0.05 phenol (1 M H ₂ SO ₄)	8	0.01	0.1	275	0.24	~13
h	NaBrO ₃ + 0.025 MnSO ₄ + 0.375 MA (1.2 M H ₂ SO ₄)	12	0.05	0.12	266	1.54	5.0
i	0.0675 NaBrO ₃ + phenol (α -peak; 1 M H ₂ SO ₄)	8	0.0075	0.0605	267	0.25	1.6
k	0.0675 NaBrO ₃ + gallic acid (γ -peak; 1.5 M H ₂ SO ₄)	7	0.005	0.03	318	0.79	5.4
l	0.0065 KMnO ₄ + MA (H ₂ O)	6	0.01	0.07	318	0.73	9.3
m	KBrO ₃ + 0.053 KBr + 0.0017 CeCl ₃ + 0.375 MA (1.5 M H ₂ SO ₄)	11	0.06	0.15	310	0.44	~43 (?)

^a MA = malonic acid; θ = DTA temperature difference; $C_{0(rat)}$ = ratio of maximum over minimum concentration, cf. last column; T_{av} = abs. average temperature.

^b Numbers = molarity of constant component.

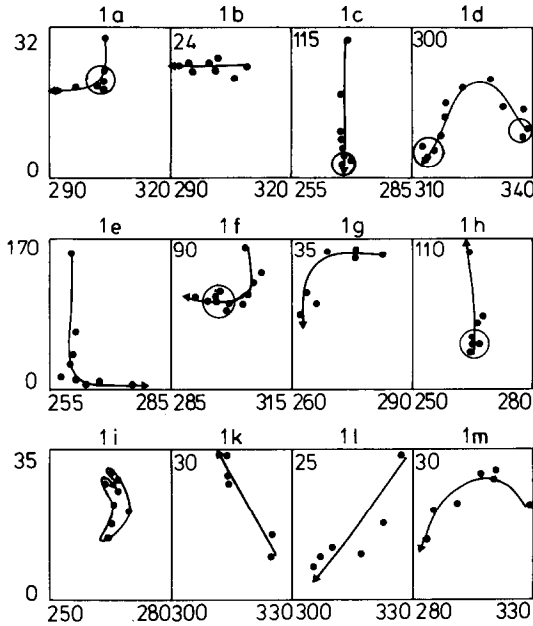


Fig. 1. Experimental T_0/θ_{rel} plots for different example series. Scales: $T_{0(max)} - T_{0(min)} = 30$ K; $\theta_{rel} = 0$ corresponds to the T_0 axis. The systems studied are listed in Table 1. In crowded regions, not all points due to experiments are presented; e.g., in the circles indicating the converging points.

heating rate) than by the concentration itself; this is because for a bimolecular reaction the rate is given by the product of the varied reactant concentrations, the A factor and a negative exponential term based on the reciprocal temperature. For an advantageous discussion of the variations of the measured variables, a correspondence to a unique concentration ratio (1 : 10) is desirable, and therefore the ratios $\log(\theta_{(max)}/\theta_{(min)})/\log(c_{0(max)}/c_{0(min)})$ and $(T_{0(max)} - T_{0(min)})/\log(c_{0(max)}/c_{0(min)})$ were considered for the particular series (the subscripts (max) and (min) refer to the highest and lowest values selected for the series). But even these “damped” ratios, given in Table 1, show extreme differences for the various series studied.

It should be mentioned that taking the peak temperatures or final temperatures often leads to similar temperature/height plots. This may offer advantages if the estimation of the T_0 values is difficult, as for an early start of a reaction directly after a freezing point. On the other hand, this observation confirms the expectation that the selected value of the sensitivity limit χ is not critical for the utility of the new diagram.

T_m values are influenced by reaction heat, and the accuracy of the T_e values may suffer from an approach to the boiling point, causing an uncertainty of the baseline [4].

DISCUSSION

On a first view on Fig. 1, the very different T_0/θ_{rel} plots imply basic differences in the prevailing kinetics.

For simplification, in the following rather theoretical discussion, the more complicated DTA curves may be replaced by the corresponding rate curves, since the features of the correlation plots usually depend much more on the type of kinetics than on the temperature dependence of heat-conduction parameters [6,10]. The directions of the height shifts are influenced by the method used since the indicative stoichiometric coefficients inside a reaction scheme may show different values or even signs. Deviations must occur for DTA in the case of strong thermal feedback, resulting in an additional increase of θ_{rel} and a strengthened negative temperature shift.

First-order reaction (= type 1) [8,14]

The relative signal height is given by

$$v_{\text{rel}} = \frac{v_m}{a_0} = \frac{1}{eu_m} = \text{constant} \quad (1)$$

since the specific temperature difference

$$u_m = \frac{E/R}{\phi(\ln k_\infty + \ln u_m)^2} \quad (2)$$

is independent of the concentration. On the other hand, the initial temperature is given by

$$T_0 = \frac{E/R}{\ln k_\infty + \ln u_m - \ln \chi} \quad (3)$$

where χ represents the relative sensitivity limit ($\approx 0.5\%$). Therefore, both quantities remain constant, and the T_0/v_{rel} plot is simply a point in the T_0/v_{rel} plane (Fig. 2).

For the benzenediazoniumsulfate system (series a/b in Table 1; ref. 15), the standardized initial temperatures and heights of Table 1, plotted in Fig. 1a, seem to correspond to a curve rather than to an exact point (cf. ref. 2). However, a total of five points from experiments where concentrations $0.05 < a_0 < 0.4 \text{ M}$ are located inside the circle shown.

Second-order reaction $A + A \rightarrow \text{products}$ (= type 2) [6,8]

Here, the conditions become more complicated, because the initial temperature is now reduced with increasing initial concentration (term $\ln a_0$)

$$T_0 = \frac{E/R}{\ln k_\infty + \ln u_m - \ln \chi + \ln 2 + \ln a_0} \quad (4)$$

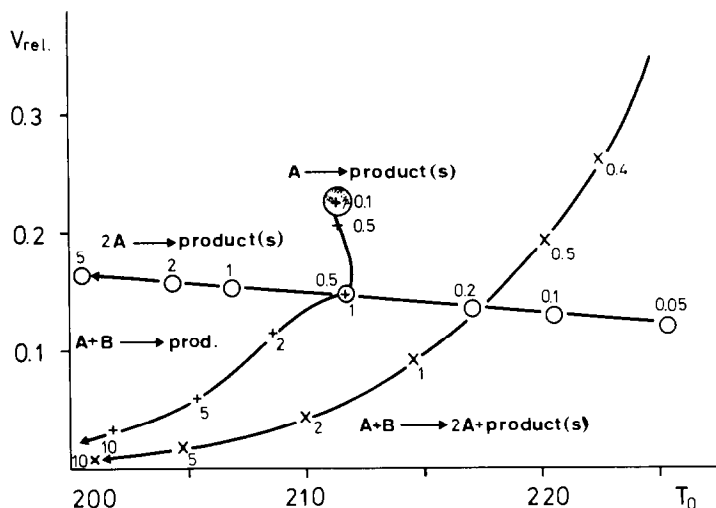


Fig. 2. Theoretical T_0/v_m plots for the fundamental one-step reactions with activation parameters $E = 15 \text{ kcal mol}^{-1}$, $k_\infty = 10^{12} \text{ min}^{-1}$ or $1 \text{ mol}^{-1} \text{ min}^{-1}$. The numbers near the presented points on the curve are the starting concentrations a_0 of species A, used for the respective simulations.

whereas v_{rel} remains nearly constant. The result is a slightly inclined straight line as in Fig. 2 going from right to left with increasing starting concentration.

Figure 1b is an experimental example for such a plot, although even in that case (decomposition of benzenediazonium sulfate after its formation from an equimolar ratio of sodium nitrite and aniline at ice temperature) a unimolecular course had been expected. We assume an incomplete formation of the diazonium salt, leading to excess reactant, such as nitrous acid, which may undergo a bimolecular process with the diazonium salt.

Bimolecular reaction $A + B \rightarrow \text{product}(s)$ (= type 3) [5]

Unlike type 2, the signal height now becomes dependent on two reactant concentrations. As limiting cases, the constant signal height of a first-order process (= pseudo unimolecular reaction) or the value of zero must appear, as is considered by the following empirical approximation for $b_0 = \text{constant}$,

$$v_{\text{rel}} \approx \frac{\text{const.}}{u_m} \arctan a_0 \quad (5)$$

The initial temperature becomes

$$T_0 \approx \frac{E/R}{\ln k_\infty + \ln u_m + a \ln a_0 + b \ln b_0 - \ln \chi} \quad (6)$$

where a_0 (initial concentration), for the varied educt; b_0 , for the constant

educt; a , b are constants: $a = 0.75$; $b = 0.19$ for excess a_0 [6]. Then, the parametric plot is for $b_0 = \text{constant}$

$$v_{\text{rel}} \approx \frac{\text{const.}}{u_m} \arctan \frac{0.00083}{k_{\infty} \exp(-E/T_0) a_0^a} \quad (7)$$

This equation corresponds to a primarily vertical, descending curve as in Fig. 2 (increase of a_0 from right to left) which evolves from a “pseudounimolecular” source point; for $a_0 = b_0$ the curve passes the equivalence point, for $a_0 > b_0$ it turns abruptly left, and, finally, converges towards the T_0 axis.

Bimolecular autocatalytic reaction $A + B \rightarrow 2 B$ (+ product(s)) (= type 4)

Although non-elementary, this type of reaction [5] is observed in many interesting processes, e.g., in oscillating reactions [1,2,4]. However, it is not possible to derive a mathematical expression for the reaction rate as a function of time. Thus, a series of model curves was generated by numerical integration for different values of a_0 , and the data of these theoretical curves (activation parameters: $E = 15 \text{ kcal mol}^{-1}$, $\log A = 10.5$) were plotted as for the experimental series.

From the diagrams a_0/T_0 and a_0/v_{rel} the following empirical relationships were obtained

$$\log v_{\text{rel}} \approx l - r \log a_0 \quad (8)$$

$$T_0 \approx T_c - s \log a_0 \quad (9)$$

l , r and s are constants, and one obtains for the plot

$$v_{\text{rel}} \approx v_c e^{\beta(T_0 - T_c)} \quad (10)$$

with $\beta = r/s$, $v_c = e^l$. The corresponding curve (Fig. 2) increases steeply with advancing T_0 (negative temperature shift as for types 2 and 3).

Two or more processes





For complex reactions, the derivative of a physical quantity of measurement can be represented by the contributions of elementary steps, which may be observed by means of corresponding indication parameters, λ_i , such as heat of reaction, differences of extinction coefficients, etc. [2,7,8,16].

A common feature of types 2–4 is that for an increase of a_0 , a movement from the right margin to the left occurs in Fig. 2. In complex, practical cases, this negative temperature shift is preferred, but a minority of cases show no such shift or a reverse one (Fig. 1a, e, i, m). Obviously, for an isolated peak, the latter indicates an inhibition effect which may be caused by consumption of reactant in a previous reaction step.

There are also examples for both directions of signal height shift: up or down (or even constant). For a set of reactions, such a shift is not exclusively

TABLE 2
Some reaction schemes (yielding one peak) and respective concentration codes for initial temperature and relative signal height

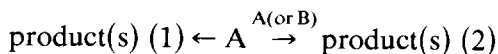
Abbr.	Reaction scheme	Data ^a	Sequential code for a_0 increase ^b		Schematic plot
			T_0	V_{rel}	
<i>Isolated</i>					
1	A → (product(s))	15, 12, 10	c	c	●
2	A + A →		-	+(nearly c)	↓
AB	A + B →		c c -	c - - 0	
1a	A + B → B + B + ...		- -	- - 0	
P_{1a}	A → B A + B →	15, 12, 10 18, 14, 5	c - + c	c c - c	
P_{2a}	A + A → B A + B →	15, 12, 10 17, 13, 15	- - c - -	c + c + c	
P_{1AB}	A → A + B →	11, 8, 15 15, 12, 10	c(+)-(-)+c	c - c + c	

G_{12}	$A \rightarrow B+B$	15, 12, 10	$c-(c)+$	$c-c-0$	
	$B+B \rightarrow A$	18, 14.8, -10			
P_{12}	$A \rightarrow$	15, 12, 10	$c(+)-$	$c-c$	
	$A+A \rightarrow$	10, 6, 20			
Overlapped	$A \rightarrow Q$	15, 12, 10	$c-(c)-(c)$	$c-c+(c)$	
	$A+A \rightarrow R$	10, 10, 15			
	$Q \rightarrow S$ (fast)	14, 13, 18			
	$Q+Q \rightarrow T$ (fast)	10, 11.3, 24			
	$A+B \rightarrow$	15, 9, 0.3	$c-?--(c)$	$(c)-c$	
	$B \rightarrow$	14, 8, 0.5			
	$A+C \rightarrow 2A+P$ (fast)	17, 12.5, 1			

^a Activation energy (kcal mol⁻¹), (logarithmic) frequency factor (min⁻¹ or l mol⁻¹ min⁻¹), weight factor, λ , respectively.

^b Symbols in order of increasing a_0 in a series: c = constant; $+$ = increasing; $-$ = decreasing; 0 = converges towards zero (no signal!). (E.g., “ $-c+$ ” means “decreasing” for low, “constant” for medium and “increasing” for high concentrations a_0 of reactant A.) The codes are the results of computer simulations; in general, they may be transferred to other data sets, especially if the order of the activation energies of the steps remains unchanged (cf. ref. 3); restrictions have to be considered for the signal heights (see text). The peak studied is considered as positive, and an alternation of the sign of the weight factors must be absent for concurrent reactions.

based on the kinetic scheme, but also on the fact that for DTA, endothermic and exothermic processes, possessing positive or negative λ_i parameters, are possible in one reaction mechanism. Analogous sign changes may occur in spectroscopic measurements [7] (λ_i = change of extinction coefficient), conductometry, etc., but not in normal TG. Hence, a vertical movement may be distinguishable between types 1 and 2 or 3, but for complex reactions, the direction of the v_{rel} shift is not necessarily a good criterion; it is advisable instead to distinguish between either movement in any direction or invariability [3,4]. Thus, for competing processes of different order



which represent building blocks for a complicated mechanism, there must be a stop of the v_{rel} shift both for sufficiently low or high a_0 values, because independently of the signs and values of the λ_i parameters, an asymptotic elementary behaviour due to types 1 or 2 has to prevail.

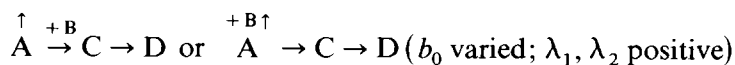
In many examples of concentration series both T_0 and θ_m remain constant over a certain period but not necessarily at the limits of the whole concentration interval (cf. 1b, 1d, 1f and 1h in Fig. 1); such stationary points indicate first-order steps in branchings, so that possibly more than two processes have to be considered [2,3,13].

On the other hand, the often observed invariability of only one of the two values can be deduced from the above elementary cases. An approximately constant relative height refers to a second-order behaviour, whereas a constant T_0 suggests that a bimolecular reaction with a deficiency of the reactant varied is rate-determining.

A corresponding plot type, often observed, is a rectangular one (e.g., Fig. 1e–g) which signals a change of rate control usually caused by an incipient excess of the reactant varied (cf. bimolecular reaction in Fig. 2).

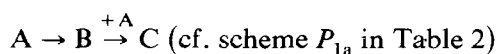
Isolated and overlapped peaks

For an isolated peak, a general discussion of the phenomena for equal λ_i 's has been performed earlier [2,7,8,16]. For an increase of component B, an exclusively vertical movement is observed, e.g., for the T_0/v_{rel} point of the second peak of mechanisms such as



(upwards) (downwards)

or, in a certain range, even for the single peak of the simplest both competitive and consecutive scheme



In general, the onset temperature shifts must depend on the type of combination of competing reactions which is directly responsible for the isolated peak (= temporary reactions) whereas the height shift depends, in addition, on the previous reactions (= kinetic history) [2,4,7,8].

When considering such overlapped peaks where the temporary reactions become fast compared to the previous reactions, then the situation is changed: indeed, the height shift remains dependent on both previous and temporary reactions, representing a kind of weighted mean of the indication parameters, λ_i , and the kinetic contribution of the participating steps. However, the initial temperature T_0 of the merged peak is no longer related to the originally "temporary" reactions; T_0 now depends exclusively on the initiating step of the previous reactions, i.e., the latter becomes rate-determining at the onset.

Therefore, only part of the information on the subsequent fast reactions will be retained in the signal height shift, which involves kinetics as well as method-dependent weight parameters, λ_i . However, the interpretation of such overlapped peaks is rather complicated compared to isolated peaks, and Table 2 may be seen as an attempt to present the type of kinetics to be deduced from the behaviour of the signal.

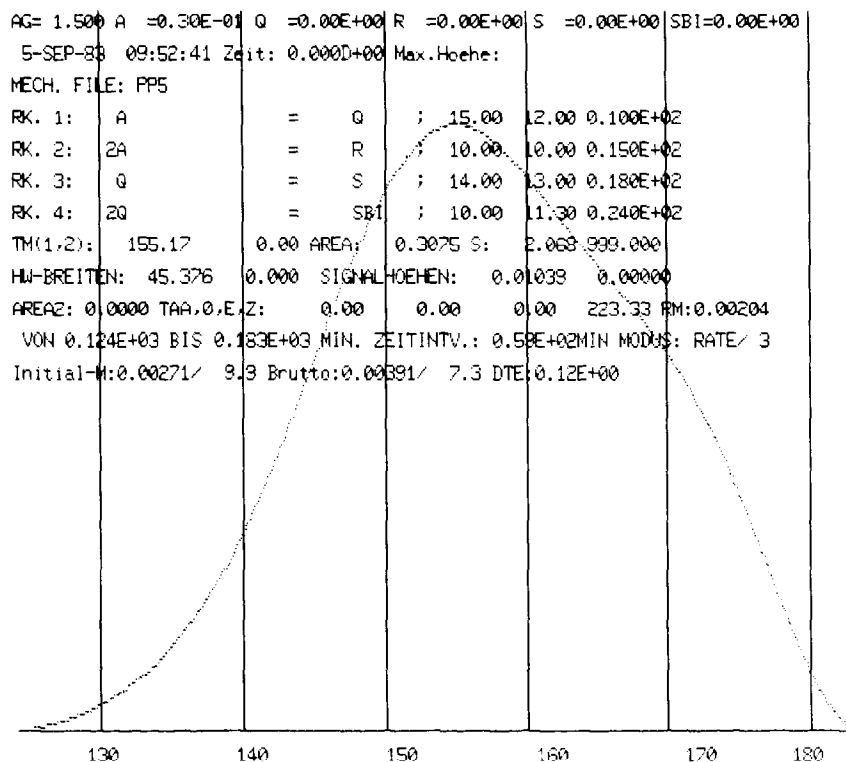
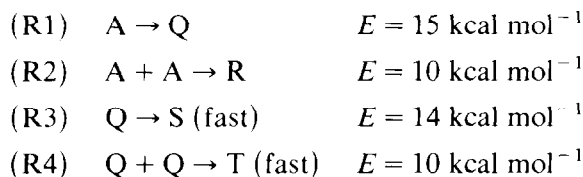


Fig. 3. Simulated rate curve for the four-step mechanism in the text (computer printout).

Theoretical example

The following mechanism, a sequence of two mixed-order branchings, was chosen as a test object for the interpretation



In a preliminary study, we omitted reactions (R3) and (R4), and assumed the A-factors $k_{\infty 1} = 10^{12} \text{ min}^{-1}$, $k_{\infty 2} = 10^{10} \text{ l mol}^{-1} \text{ min}^{-1}$ and the indication (weight) parameters $\lambda_1 = 10$, $\lambda_2 = 15$. Then, the generation of the signal curves by numerical integration (cf. Fig. 3) reveals one peak only. The T_0/v_{rel} -plot (Fig. 4) shows a source point (first order) for small a_0 's (< 0.005) and a limiting straight line (second order) for large a_0 's (> 0.1 ; cf. Fig. 2).

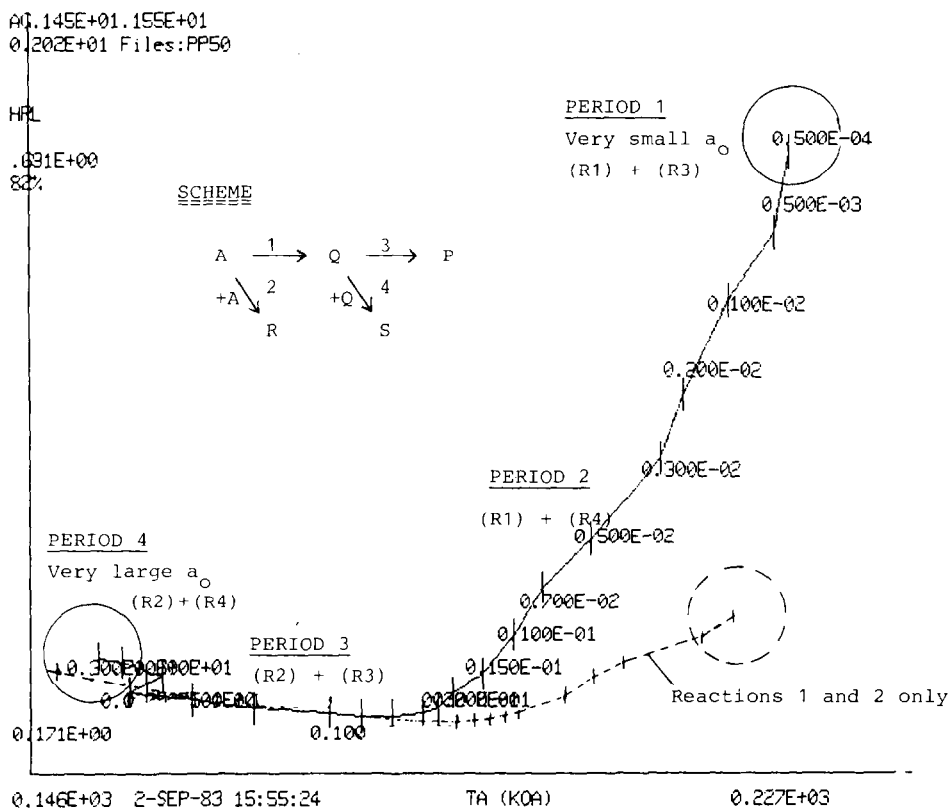


Fig. 4. Theoretical T_0/v_m plots for the mechanism in the text (cf. Fig. 3) both for presence and absence of reactions (R3) and (R4) (computer printout; cf. Table 3). The concentrations corresponding to the respective points are identical in both branches.

TABLE 3
Reaction rates and rate-determining steps for different concentrations in the four-step scheme (cf. Figs. 3-5 and text)

Period (Fig. 4)	T (K)	a_0 (M)	k_1 (s^{-1})	k_2 ($l \text{ mol}^{-1} s^{-1}$)	k_3 (s^{-1})	k_4 ($l \text{ mol}^{-1} s^{-1}$)	$[Q]_{\text{stat}}^a$ ($l \text{ mol}^{-1} s^{-1}$)	$\frac{k_2 a_0}{k_1}$	Rate- det. step	$\frac{k_4 [Q]_{\text{stat}}}{k_3}$	Rate- det. step
1	221	0.0001	2.3×10^{-5}	0.0021	2.4×10^{-3}	0.43	9.3×10^{-7}	0.092	R1	1.8×10^{-4}	R3
2	201	0.003	8.1×10^{-7}	2.2×10^{-3}	9.8×10^{-5}	0.044	2.4×10^{-5}	8.24	R2	0.0108	R3
	197	0.01	3.8×10^{-7}	1.3×10^{-3}	4.8×10^{-5}	0.027	9.0×10^{-5}	35.4	R2	4.95	R4
3	185	0.1	3.1×10^{-8}	2.5×10^{-4}	4.4×10^{-6}	0.0051	4.6×10^{-4}	80.9	R2	0.49	R3
4	155	0.5	1.2×10^{-11}	1.3×10^{-6}	3.0×10^{-9}	2.6×10^{-5}	4.2×10^{-4}	5.7×10^4	R2	3.63	R4

^a According to Bodenstein's principle, the stationary concentration of Q is given by

$$[Q]_{\text{stat}} = \frac{1}{2} \left(\sqrt{\left(\frac{k_3}{k_4} \right)^2 + 4 a_0 \frac{k_1}{k_2} - \frac{k_3}{k_4}} \right).$$

Now we complete the mechanism by adding reactions (R3) and (R4) and select as the respective data $k_{\infty 3} = 10^{13} \text{ min}^{-1}$, $\lambda_3 = 18$, $k_{\infty 4} = 10^{11.3} \text{ l mol}^{-1} \text{ min}^{-1}$ and $\lambda_4 = 24$, which means that these processes are fast compared to (R1) and (R2) at unit concentrations of species A and Q (Table 3). Figure 3 shows an example of a computer printout of a theoretical rate curve.

Evaluation of many such theoretical curves of the concentration series ($10^{-5} < a_0 < 30 \text{ M}$) gives a T_0/v_{rel} -plot distinctly different from the plot of the pre-study (Fig. 4): although we have again a source point and, later, a convergence line, the respective signal heights are increased by a factor of ~ 4 because of the additional weight parameters λ_3 and λ_4 . Further, there is a decrease of the (positive) slope beginning for $a_0 \approx 0.003$, which obviously signals the interference of the fast second-order reaction (R4) during the remaining influence of reaction (R3) (see Table 3). However, on a further increase of the initial concentration ($0.02 < a_0 < 0.2$), a second, intermediate straight line signals the newly increasing dominance of reaction (R3), whilst reaction (R2) suppresses the unimolecular reaction (R1) completely. Finally,

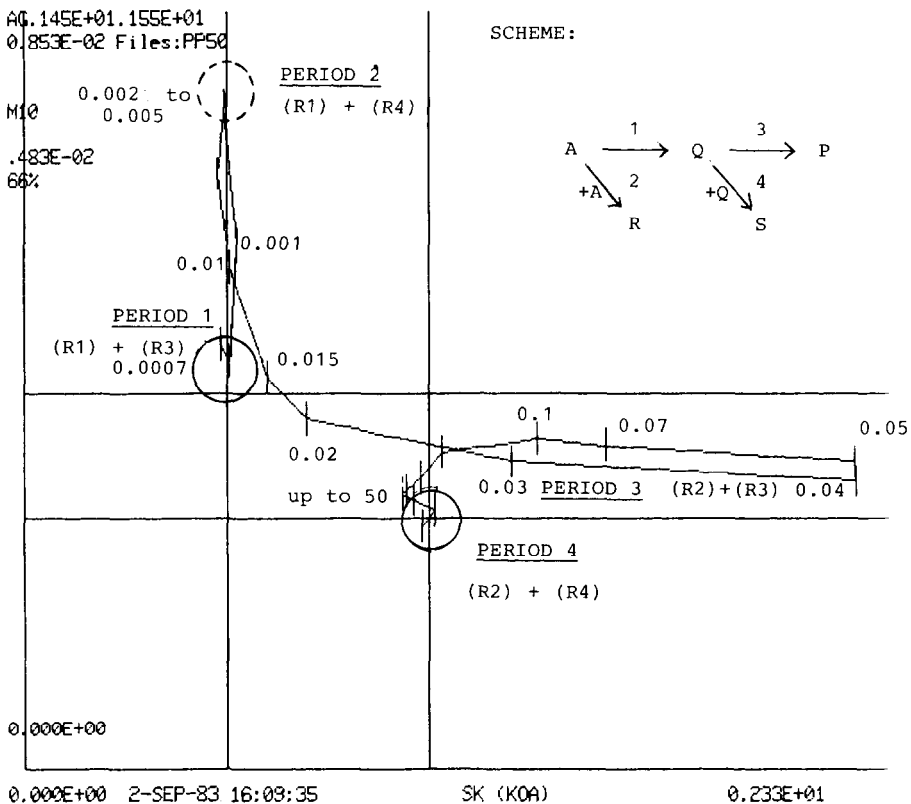


Fig. 5. Mechanistic initial diagram (computer printout of the series of Fig. 4). Abscissa: shape index; ordinate: reaction type index referred to first order of the adapted initial reaction. Supplementary numbers: cf. Fig. 2.

the plot differs from this line, signalling a remaining participation of reaction (R4), again dominating over reaction (R3).

Hence, the plot features reflect the transfer of signal control from one reaction pair to the other, but the special indications of the finally increasing dominance of the fast reaction (R4) are rather poor because of the suppression of the kinetic flux in reaction (R1). In practical experiments, such indications may be often concealed in error limits.

In contrast, the mechanistic S/M-diagram should be much better able to reveal the intermediate control of the kinetics by the particular fast steps, as is evident from Fig. 5.

CONCLUSIONS

Compared to the diagnostic value of the mechanistic indices, an interpretation of relative signal height and initial temperature shifts should be less effective [1,3], partially because the correlation of the signal height to the reactant concentration involves method-depending parameters which restrict the purely kinetic view. However, the small effort necessary for gaining these primary data often compensates for this deficiency, especially for isolated signals as in ref. 4, if the error limits are kept small by projecting a sufficient size of the series. For each rate-determining or even signal-influencing step in the mechanism, at least 3–5 experiments with different initial concentrations should be taken into consideration.

If fast steps are involved, additional information on non-rate-determining steps may be obtained (cf. reaction (R4) of the theoretical model); then the intrusion of the λ_i parameters may even be advantageous [8], because the diagram separates two points of view, presenting pure kinetic relationships [5] in the horizontal, but method-dependent kinetic relationships in the vertical direction. Additional comparative computer simulations may be very helpful in subsequent investigations related to this field.

On the basis of these concepts, we intend to discuss some special reactions in detail.

ACKNOWLEDGEMENTS

I am grateful to Mrs. B. Pirke and Mrs. G. Mummerz for performing the DTA measurements and assisting me in data evaluation and compilation.

REFERENCES

- 1 E. Koch, *Thermochim. Acta*, 56 (1982) 1.
- 2 E. Koch, *Angew. Chem.*, 95 (1983) 185; *Angew. Chem. Int. Ed. Engl.*, 22 (1982) 225.

- 3 E. Koch, *Thermochim. Acta*, 49 (1981) 25.
- 4 E. Körös and E. Koch, *Thermochim. Acta*, 71 (1983) 287.
- 5 R. Schmid and V.N. Sapunov, *Non-formal Kinetics*, Verlag Chemie, Weinheim, 1982, Ch. 4, and pp. 54–59.
- 6 E. Koch and B. Stalkerieg, *Thermochim. Acta*, 27 (1978) 69; *J. Therm. Anal.*, 17 (1979) 395.
- 7 E. Koch, in E. Marti, H.R. Oswald and H.G. Wiedemann (Eds.), *Angewandte Chemische Thermodynamik und Thermoanalytik*, Birkhäuser, Basel, 1979, pp. 210–215.
- 8 E. Koch, *Non-isothermal Reaction Analysis*, Monograph, Academic Press, London, 1977, Chaps. 3, 4, 6, 8.
- 9 E. Koch, *Chem.-Ing.-Tech.*, 37 (1965) 1004.
- 10 E. Koch, B. Stalkerieg and L. Carlsen, *Ber. Bunsenges. Phys. Chem.*, 83 (1979) 1238.
- 11 J. Steiner, Y. Termonia and J. Deltour, *Anal. Chem.*, 44 (1972) 1906.
- 12 J.H. Flynn, in S.W. Shalaby (Ed.), *Thermal Methods in Polymer Analysis*, Franklin Inst. Press, Philadelphia, PA, 1978.
- 13 E. Koch, *Angew. Chem.*, 85 (1973) 381; *Angew. Chem. Int. Ed. Engl.*, 12 (1973) 381.
- 14 E. Koch and B. Stalkerieg, *Thermochim. Acta*, 17 (1976) 1.
- 15 R.L. Reed, L. Weber and B.S. Gottfried, *Ind. Eng. Chem. Fundam.*, 4 (1965) 38.
- 16 G. Kluge, H. Eichhorn, K. Heide and M. Fritsche, *Thermochim. Acta*, 60 (1983) 303.